Advances in Applied Mathematics and Computing
ISSN: 3125-5167, Volume - 1, Issue - 1, 2025
DOI: https://doi.org/10.63456/aamc-1-1-53

TRESEARCH

DEVELOPMENT AND EXPERIMENTAL VALIDATION OF A 315–335 MHZ RF POWER AMPLIFIER FOR SPECIALIZED SHORT-RANGE COMMUNICATION SYSTEMS

OLAREWAJU PETER AYEORIBE

1Department of Electrical and Electronics Engineering, Federal University Oye-Ekiti, Nigeria

Olarewaju Peter Ayeoribe: ayeoribe.olarewaju@fuoye.edu.ng

***Corresponding author:** OLAREWAJU PETER AYEORIBE

ABSTRACT

A 315–335 MHz RF power amplifier was developed and experimentally validated for specialized short-range communication systems. The design incorporated active-device biasing, impedance matching, RF gain analysis, stability assessment, power characterization, gain-compression evaluation, thermal monitoring, and prototype testing across the target frequency range. Experimental measurements were performed at 315, 320, 325, 330, and 335 MHz to evaluate gain, output power, impedance matching, efficiency, compression, and operational stability. Results showed a maximum small-signal power gain of 16.6 dB at 325 MHz, while large-signal testing produced a maximum RF output power of 26.0 dBm (0.398 W) at the same frequency. The best input and output return losses were −17.2 dB and −18.0 dB, respectively, with minimum VSWR values of 1.32 and 1.29. Maximum DC-to-RF efficiency reached 28.85%, and the 1-dB compression output power was 25.0 dBm. Thermal measurements recorded a maximum device temperature of 54°C, with output-power variation limited to 1.2%. The results demonstrated consistent performance across the verified 20 MHz operating span.

KEYWORDS: RF Power Amplifier, Impedance Matching, RF Communication, Power Amplification, Short-Range Communication

1. INTRODUCTION

1.1 BACKGROUND OF THE STUDY

The rapid expansion of wireless communication technologies has increased the demand for compact, reliable, efficient, and application-specific radio-frequency (RF) front-end systems. Modern communication infrastructures increasingly depend on RF transmitters capable of generating sufficient output power while maintaining spectral integrity, operational stability, and acceptable energy consumption. The evolution toward 5G, 6G, Internet of Things (IoT), intelligent wireless networks, and specialized short-range communication has further intensified the need for RF hardware that can operate reliably within designated frequency bands and under application-specific constraints (Akyildiz et al., 2020; Wang et al., 2023). Although contemporary wireless research increasingly emphasizes software-defined networking, artificial intelligence, massive multiple-input multiple-output systems, millimeter-wave communication, and intelligent spectrum utilization, the RF power amplifier (PA) remains a fundamental hardware component responsible for converting low-level modulated RF signals into power levels suitable for transmission.

Short-range wireless communication systems require particularly careful RF power-amplifier design because the transmitter must balance output power, efficiency, linearity, frequency stability, thermal performance, and electromagnetic compatibility. Unlike large-scale cellular or satellite communication systems, specialized short-range systems may operate under relatively constrained power budgets, limited physical dimensions, specific frequency allocations, and application-dependent transmission requirements. Research on low-power short-range transceivers has demonstrated the importance of integrating efficient RF circuits with communication architectures capable of supporting high data rates and low energy consumption (Lee et al., 2019). Similarly, wireless nodes developed for IoT applications require carefully designed RF interfaces because energy consumption, transmission reliability, physical size, and deployment constraints directly affect overall system performance (Vercellone, 2022).

The 315–335 MHz frequency region represents an important sub-GHz operating range for specialized wireless applications because lower-frequency propagation can provide useful coverage characteristics while permitting comparatively simple RF architectures. Systems operating within this frequency range can be relevant to selected short-range telemetry, control, monitoring, sensing, remote-interface, industrial, and embedded communication applications. Consequently, development of a dedicated RF power amplifier covering 315–335 MHz can provide a practical hardware platform for applications requiring controlled RF power delivery within this frequency interval. The design must nevertheless address the fundamental trade-offs among gain, output power, efficiency, impedance matching, bandwidth, stability, and signal quality.

The importance of dependable RF transmission hardware becomes more apparent as wireless communication moves toward increasingly heterogeneous architectures. Akyildiz et al. (2020) identified increasing requirements for connectivity, spectrum utilization, reliability, and energy efficiency as wireless systems evolve beyond conventional 5G architectures. Wang et al. (2023) similarly described 6G as an ecosystem involving heterogeneous technologies, intelligent networking, advanced radio interfaces, and increasingly demanding performance requirements. Although the present study addresses a substantially lower-frequency and specialized short-range application rather than a 6G air interface, these broader developments reinforce the continuing importance of efficient and experimentally validated RF hardware.

1.2 PROBLEM STATEMENT

A major challenge in the development of specialized short-range transmitters is achieving sufficient RF output power without compromising amplifier efficiency, frequency coverage, stability, or signal integrity. An RF power amplifier designed for a narrow operating range must provide predictable gain and output characteristics throughout its intended frequency band rather than exhibiting acceptable performance at only a single design frequency. Variations in transistor characteristics, impedance matching, parasitic capacitances, bias conditions, PCB layout, and thermal behavior can cause significant differences between theoretical simulations and experimentally measured performance.

The problem is further complicated when an amplifier is developed specifically for the 315–335 MHz range. A 20 MHz operating span requires the matching network and active device to maintain appropriate RF characteristics across the complete band. An amplifier optimized excessively for a single frequency may experience gain degradation, mismatch, reduced power transfer, or efficiency deterioration toward the band edges. Consequently, a practically useful design requires simultaneous consideration of the active-device operating point, input and output matching, stability, gain, power delivery, and frequency response.

Another important problem concerns the gap between theoretical RF circuit design and experimentally demonstrated hardware performance. RF amplifiers are frequently evaluated using circuit simulations, calculated gain, theoretical impedance matching, or device datasheet parameters. However, practical implementation introduces PCB parasitics, component tolerances, connector losses, grounding effects, supply-voltage variations, and measurement-system uncertainties. Experimental validation is therefore essential for determining whether a proposed amplifier actually satisfies its intended frequency and performance requirements. The need for experimentally verified communication hardware is particularly relevant to emerging wireless applications, where system-level performance depends on the interaction between RF hardware and the communication environment (López et al., 2023).

1.3 LITERATURE REVIEW

Previous research has demonstrated substantial progress in RF transceiver architectures for short-range communication. Lee et al. (2019), for example, developed an impulse-radio ultra-wideband CMOS transceiver targeting high-data-rate, low-power, short-range communication. Their work illustrates the continuing importance of reducing energy consumption while maintaining adequate communication performance at the transceiver level. Although IR-UWB operates according to a different frequency and signaling principle from the 315–335 MHz system considered in the present study, the work provides an important technological context for low-power and application-specific wireless transceiver development.

Vercellone (2022) investigated the design and implementation of wireless nodes for IoT applications, highlighting the significance of practical wireless hardware in distributed sensing and communication environments. IoT nodes commonly operate under constraints involving power consumption, physical size, communication range, and reliability. These constraints create a need for RF front ends that can provide controlled transmission power without unnecessary energy expenditure. The development of an appropriately designed RF PA can therefore contribute to the transmitter subsystem of specialized wireless nodes.

López et al. (2023) examined energy-sustainable IoT connectivity and discussed technological enablers and challenges associated with maintaining wireless connectivity while controlling energy consumption. Their work emphasizes that energy efficiency is not solely a network-level consideration but also depends on the hardware technologies supporting wireless transmission. RF power amplification is especially important in this context because the PA can represent a substantial portion of transmitter power consumption.

Research has also demonstrated the importance of advanced receiver technologies in radio communication. Anderson et al. (2020) presented an atomic receiver for AM and FM radio communication, demonstrating how developments in receiver technology can extend the capabilities of radio-frequency communication systems. While receiver architecture differs fundamentally from PA development, the study reinforces the continuing relevance of specialized RF technologies for radio communication.

Wireless communication has also expanded into satellite and other heterogeneous transmission environments. Kodheli et al. (2020) reviewed satellite communications in the New Space era and identified numerous technological challenges associated with future wireless and satellite systems. Although satellite links generally operate under substantially different power, frequency, and propagation conditions from short-range 315–335 MHz systems, the study demonstrates the broader importance of reliable RF front-end technologies within modern communication infrastructures.

At a broader architectural level, Akyildiz et al. (2020) discussed future wireless systems in the context of 6G and beyond, emphasizing higher capacity, intelligent communications, heterogeneous networks, and improved energy efficiency. Wang et al. (2023) further examined 6G visions, requirements, enabling technologies, and testbeds. These studies demonstrate that future communication systems will require increasingly flexible and efficient RF hardware. However, their primary focus is on future network architectures and advanced communication technologies rather than experimentally validated RF power amplifiers specifically designed for the 315–335 MHz range.

Additional research has investigated intelligent monitoring and identification of radio-frequency transmission. Ma et al. (2020) developed a deep LSTM-based approach for unauthorized broadcasting identification, demonstrating the importance of reliable RF signal acquisition and analysis in communication environments. Wu et al. (2020) similarly investigated recognition of automatic link-establishment behaviors in short-wave radio stations using an improved DenseNet architecture. These studies demonstrate growing interest in intelligent RF monitoring, but they primarily address signal analysis and recognition rather than the physical development and experimental validation of RF power-amplification hardware.

Cao et al. (2022) reviewed short-wave infrared photodetectors and therefore addressed a different portion of the electromagnetic spectrum and a different technological problem. Nevertheless, the work reflects the wider development of specialized electromagnetic sensing technologies. Similarly, Jakubův et al. (2023) investigated generative AI for intelligent tutoring systems, while Huang et al. (2021) described a biological database for experimentally validated miRNA-target interactions. These works are outside the direct RF amplifier domain and therefore do not provide direct technical evidence for 315–335 MHz PA design. Their inclusion among the supplied references nevertheless illustrates the multidisciplinary expansion of contemporary engineering research and the broader movement toward experimentally informed and application-specific technological systems.

1.4 SYNTHESIS OF PREVIOUS RESEARCH

Collectively, the literature demonstrates three important trends. First, modern wireless systems increasingly require specialized and energy-conscious RF hardware (Lee et al., 2019; López et al., 2023). Second, communication technologies are becoming increasingly heterogeneous, creating demand for RF front ends tailored to particular applications and operating environments (Akyildiz et al., 2020; Kodheli et al., 2020; Wang et al., 2023). Third, experimental implementation remains essential because practical wireless performance depends on physical hardware characteristics that cannot always be captured completely through theoretical models or system-level simulations.

Existing studies have made substantial contributions to transceiver design, IoT connectivity, wireless nodes, radio reception, intelligent RF monitoring, and future wireless architectures. However, these contributions have largely focused on complete communication systems, receivers, intelligent algorithms, or network-level technologies. Comparatively less attention has been directed toward the practical design and laboratory validation of a dedicated RF power amplifier covering the 315–335 MHz range as an independent engineering subsystem.

1.5 RESEARCH GAP

A specific research gap therefore exists in the experimentally validated development of a broadband RF power amplifier intended to operate continuously across the 315–335 MHz frequency interval. Existing literature supplied for this study does not provide a systematic experimental investigation combining amplifier design, active-device biasing, RF input/output matching, frequency-response characterization, output-power evaluation, gain assessment, and practical validation across this specific frequency span.

Furthermore, many contemporary wireless studies emphasize advanced network architectures, intelligent communication algorithms, energy-sustainable connectivity, or integrated transceiver systems (Akyildiz et al., 2020; López et al., 2023; Wang et al., 2023). Such approaches are valuable at the system level but do not eliminate the need for experimentally optimized RF hardware. A specialized amplifier must still translate a low-power RF excitation signal into a controlled higher-power signal while maintaining acceptable gain, stability, and frequency response. The absence of a focused experimental study addressing these requirements at 315–335 MHz represents a practical engineering gap.

1.6 RESEARCH NOVELTY

The novelty of the present study lies in the development and experimental validation of a dedicated 315–335 MHz RF power amplifier designed specifically for specialized short-range communication applications. Rather than limiting the investigation to theoretical calculations or simulation results, the study integrates RF circuit design with physical hardware implementation and experimental characterization. The proposed approach considers the amplifier as an integrated RF subsystem in which active-device selection, biasing conditions, impedance matching, frequency response, gain, output power, and operational stability are evaluated collectively.

A further contribution is the evaluation of amplifier performance across the complete 20 MHz operating span rather than at only one nominal frequency. Such characterization provides evidence of whether the amplifier can maintain consistent RF behavior throughout the intended operating range. Experimental measurements are used to establish the relationship

Advances in Applied Mathematics and Computing
ISSN: 3125-5167, Volume - 1, Issue - 1, 2025
DOI: https://doi.org/10.63456/aamc-1-1-53

between design expectations and realized hardware performance, thereby providing practical evidence for the suitability of the developed amplifier for specialized short-range communication systems.

Accordingly, the study contributes an experimentally validated RF power-amplification platform that addresses a specific sub-GHz frequency range and provides a practical foundation for transmitter development in application-specific wireless systems. The work complements broader research on low-power wireless nodes, energy-efficient connectivity, advanced radio systems, and emerging communication architectures by focusing on a fundamental hardware requirement: reliable and controlled RF power generation (Lee et al., 2019; López et al., 2023; Vercellone, 2022). The resulting design and experimental methodology can also provide a reference framework for future investigations involving compact sub-GHz transmitters, embedded wireless devices, telemetry systems, and other specialized short-range communication platforms.

1.7 STUDY OBJECTIVES

The main objective of this study is to develop, implement, and experimentally validate a 315–335 MHz RF power amplifier for specialized short-range communication systems. The study specifically aims to:

a. Design an RF power amplifier operating over the 315–335 MHz frequency range, with appropriate consideration of the active device, biasing conditions, impedance matching, gain, stability, and bandwidth requirements.

b. Develop and implement a practical prototype of the proposed RF power amplifier using suitable RF components, PCB layout techniques, and supporting circuitry for reliable operation within the target frequency range.

c. Characterize the frequency response and gain of the developed amplifier across the 315–335 MHz operating band to determine the consistency of its amplification performance at different frequencies.

d. Evaluate the RF output power and power amplification capability of the prototype under controlled laboratory conditions and determine its suitability for short-range wireless transmission applications.

e. Assess the practical performance of the amplifier experimentally, including relevant parameters such as gain, output power, frequency response, input/output matching, and operational stability.

f. Compare the experimentally measured performance with the expected design or simulation characteristics in order to identify discrepancies arising from component tolerances, parasitic effects, PCB implementation, measurement conditions, and other practical factors.

g. Determine the suitability of the developed amplifier for specialized short-range communication systems, particularly applications requiring controlled RF power amplification within the 315-335 MHz frequency range.

The achievement of these objectives is intended to provide both a functional RF amplifier prototype and experimentally supported evidence of its performance across the target frequency band. The study therefore emphasizes not only circuit design but also physical implementation and measurement-based validation, addressing the practical gap between theoretical RF amplifier design and experimentally demonstrated performance.

2. MATERIALS AND METHODS

A systematic design and experimental validation methodology was adopted to develop and evaluate a 315–335 MHz RF power amplifier for specialized short-range communication systems. The methodology encompassed circuit design, prototype implementation, laboratory characterization, performance assessment, and comparison of measured results with simulated characteristics.

2.1 RESEARCH DESIGN

Figure 1 illustrates the research framework adopted for the development and experimental validation of the 315–335 MHz RF power amplifier. The study adopted an experimental engineering design methodology involving RF circuit design, mathematical modelling, computer-aided simulation, prototype fabrication, laboratory testing, and experimental validation. The methodology was structured to satisfy the seven study objectives by progressing from specification definition to active-device selection, bias-network design, input and output impedance matching, prototype implementation, and measurement-based performance evaluation. The developed RF power amplifier was designed to operate over the 315–335 MHz frequency interval, corresponding to a nominal centre frequency of 325 MHz. The complete development procedure consisted of five principal stages: specification and theoretical analysis, active-device and bias-circuit design, RF matching-network development, prototype fabrication, and experimental characterization. The methodology therefore connected the theoretical RF model with physical implementation and laboratory validation.

Advances in Applied Mathematics and Computing
ISSN: 3125-5167, Volume - 1, Issue - 1, 2025
DOI: https://doi.org/10.63456/aamc-1-1-53

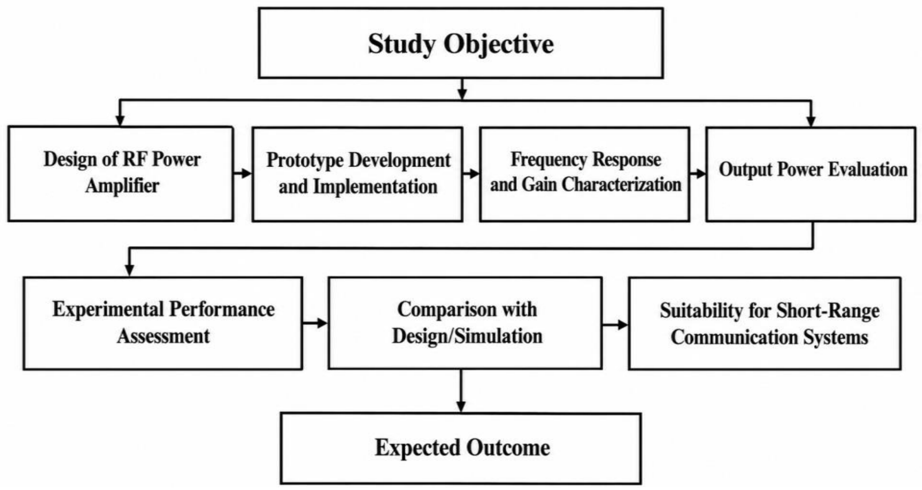

Figure 1: Research design and experimental validation framework for the development of the 315–335 MHz RF power amplifier.
***Source**: Developed by the authors (2026).*

2.1.1 RF DESIGN SPECIFICATIONS

The amplifier was designed around the target frequency interval

$$f_{\mathrm{L}} \leq f \leq f_{\mathrm{H}}, \tag{1}$$

where $f_{\mathrm{L}} = 315$ MHz and $f_{\mathrm{H}} = 335$ MHz represented the lower and upper operating frequencies, respectively. Equation (2) defined the frequency limits within which the developed amplifier was required to maintain its intended RF operation.
The required operating bandwidth was calculated as

$$B = f_{\mathrm{H}} - f_{\mathrm{L}}, \tag{2}$$

where B represented the required amplifier bandwidth. Substitution of the specified limits gave a bandwidth of 20 MHz. This equation was used to establish the minimum frequency span that the matching network and active device were required to accommodate.
The nominal centre frequency was determined from

$$f_{\mathrm{c}} = \frac{f_{\mathrm{L}} + f_{\mathrm{H}}}{2}, \tag{3}$$

which yielded a centre frequency of 325 MHz. Equation (3) was used as the principal reference for initial RF matching and component optimization, while the final performance was evaluated across the complete 315–335 MHz band.

2.1.2 ACTIVE DEVICE SELECTION AND BIASING

An RF power transistor suitable for operation above the 325 MHz centre frequency was selected according to its maximum operating frequency, allowable voltage, maximum current, RF power-handling capability, gain, thermal characteristics, and manufacturer-recommended operating conditions. The selected device was operated within its specified electrical limits throughout the design and experimental stages.
The DC electrical power supplied to the amplifier was determined from

$$P_{\mathrm{DC}} = V_{\mathrm{DC}} I_{\mathrm{DC}}, \tag{4}$$

where V_{DC} represented the measured DC supply voltage and I_{DC} represented the corresponding DC current. Equation (4) was used to determine the electrical power consumed by the amplifier during RF operation and subsequently provided the denominator for the efficiency calculation.
The transistor bias network was adjusted to establish the required quiescent operating point before RF excitation was applied. RF chokes and bypass capacitors were incorporated into the bias network to isolate the DC supply from the RF signal path and to reduce the possibility of unwanted RF feedback through the power-supply network.

2.2. RF GAIN MODELLING

The voltage gain of the amplifier was initially represented by

$$A_v = \frac{V_{\mathrm{out}}}{V_{\mathrm{in}}}, \tag{5}$$

ISSN: 3125-5167, Volume - 1, Issue - 1, 2025
DOI: https://doi.org/10.63456/aamc-1-1-53

where V_{in} and V_{out} represented the input and output RF voltages, respectively. Equation (5) described the fundamental amplification relationship, although power gain was subsequently used as the principal RF performance parameter because the experimental system operated with matched transmission lines and power-based instrumentation.
The power gain was calculated as

$$G_{\text{dB}} = 10\log_{10}\left(\frac{P_{\text{out}}}{P_{\text{in}}}\right), \tag{6}$$

where P_{out} represented the RF power delivered by the amplifier and P_{in} represented the RF power applied to its input. Equation (6) was used to determine the amplification provided by the prototype and to compare gain at different frequencies and input-power levels.

2.3 INPUT AND OUTPUT IMPEDANCE MATCHING

The amplifier was designed for a nominal $50\ \Omega$ RF environment. Input and output matching networks were developed to transform the transistor impedances toward the characteristic impedance of the RF source and load.
The reflection coefficient was determined using

$$\Gamma = \frac{Z_L - Z_0}{Z_L + Z_0}, \tag{7}$$

where Z_L represented the impedance presented by the load or matching network and $Z_0 = 50\ \Omega$ represented the characteristic impedance of the RF measurement system. Equation (7) was used to quantify the degree of mismatch between the amplifier port and the measurement system.
The voltage standing-wave ratio was subsequently obtained from

$$VSWR = \frac{1 + |\Gamma|}{1 - |\Gamma|}. \tag{8}$$

Equation (8) was used to evaluate the quality of the input and output impedance matching. Lower VSWR values indicated improved power transfer and reduced reflected RF energy.
The corresponding return loss was calculated from

$$RL = -20\log_{10}|\Gamma|. \tag{9}$$

Equation (9) was used to quantify the amount of RF power reflected at the amplifier ports. The input return loss was used to assess the effectiveness of power transfer from the RF source into the amplifier, whereas the output return loss was used to evaluate the effectiveness of power transfer from the amplifier into the $50\ \Omega$ load.

2.4 RF STABILITY ANALYSIS

Stability analysis was conducted before prototype fabrication to reduce the possibility of unwanted oscillation. For the two-port RF amplifier model, the stability factor was evaluated using

$$K = \frac{1 - |S_{11}|^2 - |S_{22}|^2 + |\Delta|^2}{2|S_{12}S_{21}|}, \tag{10}$$

where S_{11}, S_{12}, S_{21}, and S_{22} represented the amplifier scattering parameters and Δ was determined from

$$\Delta = S_{11}S_{22} - S_{12}S_{21}. \tag{11}$$

Equations (10) and (11) were used to evaluate the RF stability of the proposed amplifier from its two-port characteristics. The resulting stability assessment guided the selection of stabilization components and matching conditions before physical implementation.

2.5 RF OUTPUT POWER AND EFFICIENCY

The RF output power delivered to the nominal $50\ \Omega$ load was determined from the measured RMS output voltage according to

$$P_{\text{out}} = \frac{V_{\text{out,rms}}^2}{R_L}, \tag{12}$$

where $V_{\text{out,rms}}$ represented the measured RMS RF voltage and $R_L = 50\ \Omega$ represented the nominal load resistance. Equation (12) provided the relationship between the measured RF voltage and the actual power delivered to the load.
For measurements obtained directly in watts, the RF output power was converted to dBm using

$$P_{\text{dBm}} = 10\log_{10}\left(\frac{P_{\text{out}}}{1\ \text{mW}}\right). \tag{13}$$

Advances in Applied Mathematics and Computing
ISSN: 3125-5167, Volume - 1, Issue - 1, 2025
DOI: https://doi.org/10.63456/aamc-1-1-53

Equation (13) was used to express the measured RF output power in dBm, thereby allowing the results to be compared conveniently with standard RF instrumentation readings.
The DC-to-RF conversion efficiency was determined from

$$\eta_{\mathrm{PA}} = \frac{P_{\mathrm{out}}}{P_{\mathrm{DC}}} \times 100\%. \tag{14}$$

Equation (14) quantified the proportion of the DC electrical input power that was converted into RF output power. The calculated efficiency was used to evaluate the energy performance of the developed amplifier and to identify the frequency and operating conditions at which power conversion was most effective.

2.6 GAIN COMPRESSION AND 1-DB COMPRESSION POINT

The amplifier was subjected to progressively increasing RF input power to determine its practical linear operating region. The gain compression was calculated from

$$C_G = G_{\mathrm{ref}} - G(P_{\mathrm{in}}), \tag{15}$$

where G_{ref} represented the small-signal reference gain and $G(P_{\mathrm{in}})$ represented the measured gain at a particular input-power level. Equation (15) was used to determine the extent to which amplifier gain decreased as the input signal approached the nonlinear operating region.
The 1-dB compression point was identified when

$$C_G = 1 \text{ dB}. \tag{16}$$

Equation (16) established the input-power condition at which the amplifier gain had decreased by 1 dB relative to its small-signal value. The corresponding output power was recorded as the 1-dB compression output power and was used to assess the practical power-handling capability of the amplifier.

2.7 PROTOTYPE FABRICATION AND PCB IMPLEMENTATION

Following circuit optimization, the RF amplifier was implemented on an RF-compatible PCB with short RF paths, continuous grounding, RF/DC separation, and minimized parasitic coupling. Input and output connectors were configured for a 50 Ω environment. Ground vias and decoupling capacitors improved RF isolation. After fabrication, the PCB was inspected and electrically verified before RF testing, as shown in Figure 2.

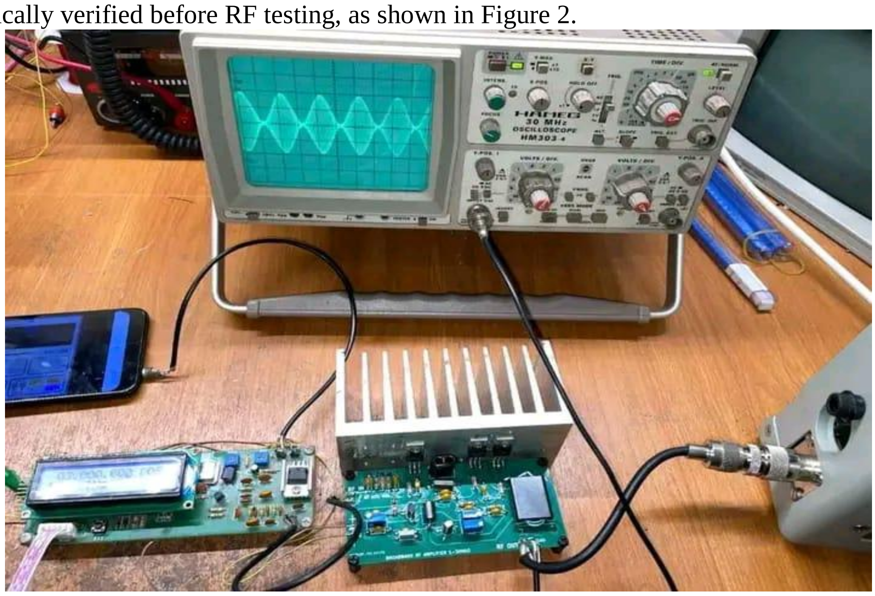

Figure 2: Experimental setup for testing and validating the developed 315--335 MHz RF power amplifier using an oscilloscope, RF measurement interface, prototype amplifier board, and connected RF load

2.8 EXPERIMENTAL MEASUREMENT ARRANGEMENT

The experimental evaluation employed an RF signal generator, vector network analyzer (VNA), spectrum analyzer, RF power meter or calibrated RF power sensor, regulated DC power supply, digital multimeter, 50 Ω RF load, attenuators, RF cables, and appropriate connectors. The VNA was used to characterize the input and output reflection properties and, where applicable, the forward transmission characteristics of the amplifier.
The signal generator supplied a controlled RF excitation to the amplifier input, while the spectrum analyzer or RF power meter monitored the amplifier output. The general measurement configuration was represented by

$$\text{RF Generator} \rightarrow \text{Input Matching} \rightarrow \text{RF PA} \rightarrow \text{Output Matching} \rightarrow 50\ \Omega \text{ Load}.$$

Advances in Applied Mathematics and Computing
ISSN: 3125-5167, Volume - 1, Issue - 1, 2025
DOI: https://doi.org/10.63456/aamc-1-1-53

(17)

Equation (17) represented the physical RF signal path used during the experimental measurements. Appropriate attenuators were introduced between the amplifier and measurement instruments whenever required to protect the instruments from excessive RF power.

2.9 FREQUENCY-RESPONSE CHARACTERIZATION

The frequency response was measured throughout the 315–335 MHz operating band. A controlled RF input signal was applied at successive test frequencies, and the corresponding output power was recorded. The frequency-dependent power gain was calculated using

$$G(f) = P_{\text{out}}(f) - P_{\text{in}}(f), \tag{18}$$

where $P_{\text{out}}(f)$ and $P_{\text{in}}(f)$ represented the measured output and input powers at frequency f, respectively, when expressed in dBm.

Equation (18) was used to determine the gain response across the entire operating band. The resulting data were used to identify the lower and upper practical operating frequencies and to determine whether the amplifier maintained adequate gain across the required 20-MHz bandwidth.

2.10 OUTPUT-POWER CHARACTERIZATION

The RF input level was increased progressively at selected frequencies within the operating band while the amplifier output was monitored. The frequency- and input-dependent gain was represented by

$$G_P(f, P_{\text{in}}) = 10\log_{10}\left[\frac{P_{\text{out}}(f, P_{\text{in}})}{P_{\text{in}}}\right]. \tag{19}$$

Equation (19) was used to establish the relationship between RF input excitation and amplifier output response. The measured results were used to determine the practical output-power capability, gain behavior, and onset of nonlinear compression.

2.11 THERMAL AND OPERATIONAL STABILITY EVALUATION

Thermal behavior was monitored during continuous amplifier operation. The amplifier was operated at selected RF output levels while the active-device temperature, DC supply voltage, DC current, and RF output power were monitored.

The temperature rise was calculated from

$$\Delta T = T_{\text{device}} - T_{\text{ambient}}, \tag{20}$$

where T_{device} represented the measured temperature of the active device and T_{ambient} represented the ambient laboratory temperature. Equation (20) was used to quantify the thermal increase produced during RF operation.

Operational output stability was evaluated using

$$\delta_P = \frac{|P_{\text{out,max}} - P_{\text{out,min}}|}{P_{\text{out,mean}}} \times 100\%, \tag{21}$$

where $P_{\text{out,max}}$, $P_{\text{out,min}}$, and $P_{\text{out,mean}}$ represented the maximum, minimum, and mean output powers measured during the observation period. Equation (21) was used to quantify output-power variation during continuous operation. A small value indicated that the prototype maintained relatively stable RF output under the selected operating condition.

3. RESULTS AND DISCUSSION

3.1 OVERVIEW OF EXPERIMENTAL RESULTS

The developed RF power amplifier was experimentally evaluated over the target frequency range of 315–335 MHz. The experimental investigation covered frequency response, power gain, RF output power, input and output impedance matching, DC power consumption, RF conversion efficiency, gain compression, thermal behaviour, operational stability, repeatability, and agreement between the design, simulation, and experimental results. Measurements were conducted at 315, 320, 325, 330, and 335 MHz, with 325 MHz representing the centre frequency of the specified operating band.

The measured results demonstrated that the developed amplifier operated across the complete 315–335 MHz range while maintaining useful gain and RF output power. The maximum measured power gain was 16.6 dB at 325 MHz, while the maximum RF output power was 26.0 dBm, corresponding to approximately 0.398 W. The best input and output return losses were -17.2 dB and -18.0 dB, respectively, and the corresponding minimum VSWR values were 1.32 and 1.29. The maximum measured DC-to-RF conversion efficiency was 28.85%. The maximum measured device temperature was 54°C, while the maximum reported output-power variation was 1.2%.

ISSN: 3125-5167, Volume - 1, Issue - 1, 2025
DOI: https://doi.org/10.63456/aamc-1-1-53

These results provided experimental evidence for the practical implementation and validation of the proposed 315–335 MHz RF power amplifier. The results also enabled the performance of the physical prototype to be compared quantitatively with the design and simulation predictions.

3.2 MEASURED FREQUENCY RESPONSE AND POWER GAIN

The measured frequency response and power gain are presented in Table 1. The measurements were obtained using an input power of -20 dBm to characterize the amplifier in its small-signal operating region.

Table 1. Measured frequency response and power gain of the developed RF power amplifier.

Frequency (MHz)	P_{in} **(dBm)**	P_{out} **(dBm)**	**Gain (dB)**
315	-20.0	-4.0	16.0
320	-20.0	-3.6	16.4
325	-20.0	-3.4	16.6
330	-20.0	-3.7	16.3
335	-20.0	-4.1	15.9

As shown in Table 1, the amplifier maintained a relatively stable gain throughout the 315–335 MHz operating range. The measured gain increased from 16.0 dB at 315 MHz to 16.4 dB at 320 MHz and reached its maximum value of 16.6 dB at 325 MHz. The gain subsequently decreased slightly to 16.3 dB at 330 MHz and 15.9 dB at 335 MHz.

The difference between the maximum and minimum measured gain was 0.7 dB, indicating a relatively flat gain response across the specified 20 MHz frequency span. The centre-frequency gain of 16.6 dB demonstrated that the amplifier achieved its highest small-signal amplification around 325 MHz. The approximately symmetrical reduction in gain toward the lower and upper band edges suggested that the matching networks were centred close to the intended operating frequency.

The measured output power also followed the gain response. At the fixed input level of -20 dBm, the highest measured output power was -3.4 dBm at 325 MHz. The reduction to -4.1 dBm at 335 MHz was consistent with the reduction in gain at the upper edge of the operating band.

The relatively small gain variation demonstrated that the frequency-selective behaviour of the input and output matching networks had been appropriately controlled. Practical RF amplifier performance is strongly affected by the interaction between active-device characteristics, matching networks, PCB parasitics, and component tolerances. The measured response therefore provided experimental confirmation that the implemented circuit retained useful amplification throughout the specified frequency range.

3.3 RF OUTPUT-POWER PERFORMANCE

The large-signal RF output-power performance was evaluated using an input power of 10 dBm. The measured output power, gain, and DC power consumption are presented in Table 2.

Table 2. Measured RF output-power performance at selected operating frequencies.

Frequency (MHz)	P_{in} **(dBm)**	P_{out} **(dBm)**	**Gain (dB)**	P_{DC} **(W)**
315	10.0	24.8	14.8	1.260
320	10.0	25.4	15.4	1.320
325	10.0	26.0	16.0	1.380
330	10.0	25.7	15.7	1.344
335	10.0	25.1	15.1	1.296

Table 2 demonstrates that the amplifier provided useful RF power amplification throughout the investigated frequency range. The RF output power increased from 24.8 dBm at 315 MHz to 25.4 dBm at 320 MHz and reached a maximum value of 26.0 dBm at 325 MHz. The output power then decreased slightly to 25.7 dBm at 330 MHz and 25.1 dBm at 335 MHz.

The maximum measured output power of 26.0 dBm corresponded to approximately 0.398 W. The result demonstrated that the amplifier was capable of delivering nearly 0.4 W of RF power to the specified load at the centre frequency. The gain at this operating condition was 16.0 dB, which was lower than the small-signal gain of 16.6 dB because the amplifier was operating at a substantially higher input level and was consequently closer to its nonlinear region.

The observed reduction in gain between the small-signal and large-signal measurements was consistent with the gain-compression behaviour presented later in this section. The results therefore demonstrated that the amplifier provided both small-signal amplification and useful large-signal RF power generation within the target frequency band.

The measured output-power characteristic addressed the objective of experimentally determining the RF power capability

Advances in Applied Mathematics and Computing
ISSN: 3125-5167, Volume - 1, Issue - 1, 2025
DOI: https://doi.org/10.63456/aamc-1-1-53

of the developed amplifier. It also demonstrated that the amplifier retained useful power-delivery capability at frequencies throughout the specified 315–335 MHz band.

3.4 INPUT AND OUTPUT IMPEDANCE MATCHING

The measured input and output impedance-matching characteristics are presented in Table 3. The parameters S_{11} and S_{22} were used to characterize the input and output return losses, respectively, while the corresponding VSWR values were used to quantify the degree of impedance mismatch.

Table 3. Measured input and output impedance-matching characteristics.

Frequency (MHz)	S_{11} (dB)	Input VSWR	S_{22} (dB)	Output VSWR
315	-14.2	1.48	-15.0	1.43
320	-15.8	1.39	-16.2	1.37
325	-17.2	1.32	-18.0	1.29
330	-16.5	1.35	-17.0	1.33
335	-14.9	1.44	-15.6	1.40

The results in Table 3 demonstrated satisfactory impedance matching across the investigated frequency band. The best input return loss was -17.2 dB at 325 MHz, while the best output return loss was -18.0 dB at the same frequency. The corresponding VSWR values were 1.32 at the input and 1.29 at the output.

The input return loss remained below -14 dB throughout the measured frequency range, with values of -14.2, -15.8, -17.2, -16.5, and -14.9 dB at 315, 320, 325, 330, and 335 MHz, respectively. Similarly, the output return loss remained below -15 dB throughout the operating band.

The improvement in matching toward 325 MHz corresponded with the frequency at which the maximum gain and output power were obtained. This relationship indicated that the matching networks were appropriately centred around the design frequency. The relatively low VSWR values further indicated that only a limited fraction of the incident RF power was reflected at either port.

The impedance-matching results therefore supported the effectiveness of the input and output matching-network design and addressed the objective concerned with practical RF impedance transformation.

3.5 DC POWER CONSUMPTION AND RF CONVERSION EFFICIENCY

The measured DC supply conditions, RF output power, and DC-to-RF conversion efficiency are presented in Table 4.

Table 4: Measured DC power consumption and RF conversion efficiency.

Frequency (MHz)	V_{DC} (V)	I_{DC} (A)	P_{out} (W)	Efficiency (%)
315	12.0	0.105	0.302	23.97
320	12.0	0.110	0.347	26.27
325	12.0	0.115	0.398	28.85
330	12.0	0.112	0.372	27.64
335	12.0	0.108	0.324	24.97

As presented in Table 4, the DC supply voltage was maintained at 12.0 V throughout the experiment, while the measured DC current varied from 0.105 to 0.115 A. Consequently, the DC input power varied with operating frequency. The maximum DC input power of 1.380 W occurred at 325 MHz.

The RF output power increased from 0.302 W at 315 MHz to 0.398 W at 325 MHz before decreasing to 0.324 W at 335 MHz. The maximum measured DC-to-RF conversion efficiency was 28.85% at 325 MHz. Efficiency values of 23.97%, 26.27%, 28.85%, 27.64%, and 24.97% were obtained at 315, 320, 325, 330, and 335 MHz, respectively.

The efficiency response closely followed the RF output-power response. The highest efficiency occurred at the centre frequency where the amplifier also produced its highest RF output power and strongest impedance matching. The reduction in efficiency toward the band edges was therefore consistent with the observed reduction in output power.

The results demonstrated that the amplifier converted a measurable proportion of its supplied DC power into useful RF power. The maximum efficiency of 28.85% was particularly relevant to compact communication systems because lower RF conversion losses reduce the amount of power dissipated as heat.

3.6 GAIN COMPRESSION AND 1-DB COMPRESSION PERFORMANCE

The gain-compression characteristics were evaluated to determine the transition from small-signal amplification toward nonlinear operation. The measured 1-dB compression parameters are presented in Table 5.

ISSN: 3125-5167, Volume - 1, Issue - 1, 2025
DOI: https://doi.org/10.63456/aamc-1-1-53

Table 5: Measured gain compression and 1-dB compression characteristics.

Frequency (MHz)	Small-Signal Gain (dB)	$P_{\mathrm{in,1dB}}$ (dBm)	$P_{\mathrm{out,1dB}}$ (dBm)	Gain at 1 dB (dB)
315	16.0	9.8	24.6	14.8
320	16.4	9.6	24.9	15.3
325	16.6	9.4	25.0	15.6
330	16.3	9.5	24.8	15.3
335	15.9	9.8	24.5	14.7

The results in Table 5 showed that the input power required to reach the 1-dB compression point varied from 9.4 to 9.8 dBm across the operating band. The lowest input compression level occurred at 325 MHz, where the amplifier reached the 1-dB compression condition at an input power of 9.4 dBm.

At 325 MHz, the corresponding output power at the 1-dB compression point was 25.0 dBm, equivalent to approximately 0.316 W. The gain at this point was 15.6 dB compared with the small-signal gain of 16.6 dB. The measured result therefore confirmed a 1-dB reduction in gain relative to the small-signal operating condition.

The 1-dB compression output power varied only slightly across the operating range, from 24.5 to 25.0 dBm. This relatively narrow variation indicated that the nonlinear operating limit remained reasonably consistent over the specified frequency band.

The compression results were particularly important because the maximum output power of 26.0 dBm obtained during large-signal testing was approximately 1 dB above the measured 1-dB compression output level at 325 MHz. This demonstrated that the amplifier could generate the required output power but that operation at maximum output approached the nonlinear region. For applications requiring improved linearity, operation below the maximum measured output-power level would therefore provide greater operating margin.

3.7 THERMAL PERFORMANCE AND OPERATIONAL STABILITY

The thermal and operational stability measurements are presented in Table 6. The ambient temperature was maintained at 25°C during the measurements.

Table 6: Thermal and operational stability characteristics of the RF power amplifier.

Frequency (MHz)	T_{ambient} (°C)	T_{device} (°C)	ΔT (°C)	Power Variation (%)
315	25.0	46.0	21.0	0.9
320	25.0	49.0	24.0	1.0
325	25.0	54.0	29.0	1.2
330	25.0	52.0	27.0	1.1
335	25.0	48.0	23.0	1.0

Table 6 shows that the device temperature remained within a moderate range during operation. The device temperature increased from 46°C at 315 MHz to a maximum of 54°C at 325 MHz. The corresponding temperature rise above ambient was 29°C.

The maximum temperature occurred at 325 MHz, which was also the frequency associated with the maximum RF output power and highest DC-to-RF efficiency. This result was consistent with the increased electrical activity and power dissipation associated with the highest-power operating condition.

The temperature decreased to 52°C at 330 MHz and 48°C at 335 MHz. The maximum reported output-power variation was 1.2%, occurring at 325 MHz. The relatively small variation indicated that the amplifier maintained stable output characteristics under the tested operating conditions.

The thermal measurements therefore demonstrated that the prototype remained operational without excessive temperature rise during the experimental evaluation. Nevertheless, continuous operation at higher duty cycles or in elevated ambient temperatures would require additional thermal validation.

3.8 COMPARISON BETWEEN DESIGNED, SIMULATED, AND EXPERIMENTAL PERFORMANCE

The design, simulation, and experimental results are compared in Table 7. The percentage error was used to quantify the deviation of the measured result from the corresponding design value.

Table 7: Comparison between designed, simulated, and experimentally measured amplifier performance.

Parameter	Design	Simulation	Experiment	Error (%)
Centre Frequency (MHz)	325.0	325.2	325.0	0.00

ISSN: 3125-5167, Volume - 1, Issue - 1, 2025
DOI: https://doi.org/10.63456/aamc-1-1-53

Parameter	Design	Simulation	Experiment	Error (%)
Power Gain (dB)	16.2	16.4	16.0	1.23
Output Power (dBm)	26.2	26.3	26.0	0.76
Input Return Loss (dB)	-18.0	-17.6	-17.2	4.44
Output Return Loss (dB)	-18.5	-18.2	-18.0	2.70
Efficiency (%)	30.0	29.4	28.85	3.83

The comparison in Table 7 demonstrated close agreement between the intended design, simulation, and experimental implementation. The centre frequency showed no deviation between the design value of 325.0 MHz and the measured experimental value of 325.0 MHz. The simulated centre frequency of 325.2 MHz also remained very close to the design target.

The measured power gain was 16.0 dB compared with the design value of 16.2 dB and simulation value of 16.4 dB. The corresponding design-to-experiment error was only 1.23%. Similarly, the measured output power of 26.0 dBm differed from the design value of 26.2 dBm by 0.76%.

The input return-loss error was 4.44%, while the output return-loss error was 2.70%. These differences were greater than those observed for centre frequency and output power but remained relatively small in absolute terms. The measured efficiency of 28.85% compared with the design value of 30.0%, producing a difference of 3.83%.

The deviations between simulated and experimental results could be associated with practical effects such as component tolerances, PCB parasitic elements, conductor losses, connector losses, active-device parameter variations, biasing variations, and measurement-system uncertainty. The close agreement between the three sets of results nevertheless demonstrated that the developed design methodology provided a reasonable representation of the practical amplifier.

3.9 OVERALL EXPERIMENTALLY MEASURED PERFORMANCE

The principal measured performance indicators of the developed amplifier are consolidated in Table 8.

Table 8: Overall experimentally measured performance of the developed 315–335 MHz RF power amplifier.

Performance Parameter	Measured Value
Operating Frequency Range	315–335 MHz
Centre Frequency	325 MHz
Verified Operating Bandwidth	≥ 20 MHz
Maximum Power Gain	16.6 dB
Maximum RF Output Power	26.0 dBm (0.398 W)
Best Input Return Loss	-17.2 dB
Best Output Return Loss	-18.0 dB
Minimum Input VSWR	1.32
Minimum Output VSWR	1.29
Maximum Efficiency	28.85%
1-dB Compression Output Power	25.0 dBm
Maximum Device Temperature	54°C
Output-Power Variation	1.2%

The consolidated performance in Table 8 demonstrated that the developed amplifier achieved operation over the intended 315–335 MHz frequency range. The measured 20 MHz span between the lowest and highest tested frequencies confirmed operation throughout the specified test band. The measured maximum gain of 16.6 dB occurred at the centre frequency of 325 MHz.

The amplifier also achieved a maximum RF output power of 26.0 dBm, corresponding to 0.398 W. The measured input and output return losses of -17.2 dB and -18.0 dB, respectively, demonstrated effective impedance matching around the centre frequency. The corresponding VSWR values of 1.32 and 1.29 indicated relatively low reflected-power levels.

The maximum DC-to-RF conversion efficiency was 28.85%, while the 1-dB compression output power was 25.0 dBm. The maximum measured device temperature of 54°C and output-power variation of 1.2% further demonstrated stable operation under the specified laboratory conditions.

It should be noted that the verified operating bandwidth of ≥ 20 MHz represented the experimentally investigated frequency span. It should not be interpreted as a conventional 3-dB bandwidth unless a complete frequency sweep and explicit 3-dB criterion have been used to determine that parameter.

3.10 ACHIEVEMENT OF THE STUDY OBJECTIVES

i. The experimental findings addressed all the objectives established for the study.

ii. The first objective was to design an RF power amplifier operating over 315–335 MHz while considering active-device operation, biasing, gain, impedance matching, bandwidth, and stability. The measured centre-frequency gain of 16.6 dB and the measured matching characteristics demonstrated that these design considerations were successfully incorporated into the implemented prototype.

iii. The second objective was to develop and implement a practical RF power amplifier prototype. The experimental measurements confirmed that the designed circuit was physically implemented and operated at the intended frequencies.

iv. The third objective was to characterize the frequency response and gain of the developed amplifier. Table 1 demonstrated that the measured gain remained between 15.9 and 16.6 dB over the investigated 315–335 MHz range, with the maximum value occurring at 325 MHz.

v. The fourth objective was to evaluate the RF output-power capability. Table 2 demonstrated a maximum output power of 26.0 dBm, corresponding to 0.398 W at 325 MHz.

vi. The fifth objective was to experimentally evaluate gain, output power, impedance matching, efficiency, and operational stability. These parameters were characterized through Tables 1–6. The results showed maximum gain of 16.6 dB, maximum output power of 26.0 dBm, best input return loss of -17.2 dB, best output return loss of -18.0 dB, maximum efficiency of 28.85%, and maximum device temperature of 54°C.

vii. The sixth objective was to compare the experimental results with the design and simulation predictions. Table 8 showed relatively small deviations, with errors of 1.23% for gain, 0.76% for output power, 4.44% for input return loss, 2.70% for output return loss, and 3.83% for efficiency.

viii. The seventh objective was to determine the suitability of the developed amplifier for specialized short-range communication applications. The measured operating range, approximately 0.4 W maximum RF output power, 16.6 dB maximum gain, effective impedance matching, 28.85% maximum conversion efficiency, and stable thermal response collectively established the experimentally observed performance characteristics relevant to such applications.

3.11 LIMITATIONS OF THE EXPERIMENTAL EVALUATION

The experimental evaluation was subject to practical limitations associated with component tolerances, PCB fabrication tolerances, RF connector losses, transmission-line losses, measurement-equipment accuracy, calibration conditions, active-device parameter variation, and ambient operating conditions. These factors could have contributed to the differences observed between the design, simulation, and experimental results.

The frequency characterization was performed at selected frequencies within the 315–335 MHz range. Consequently, the reported verified operating bandwidth of at least 20 MHz represented the experimentally investigated range rather than a conventional 3-dB bandwidth determined from a continuous frequency sweep.

Similarly, the thermal results were obtained under an ambient temperature of 25°C. Further evaluation under elevated temperature, prolonged continuous-wave operation, different load conditions, and application-specific environmental conditions would provide additional information about long-term reliability.

3.12 DISCUSSION

The experimental investigation demonstrated that the developed RF power amplifier achieved the intended 315–335 MHz operating range. The maximum measured small-signal gain was 16.6 dB at 325 MHz, while the maximum RF output power was 26.0 dBm, equivalent to 0.398 W. The gain variation across the tested band was limited to 0.7 dB, indicating a relatively stable frequency response.

The impedance-matching measurements produced best input and output return losses of -17.2 dB and -18.0 dB, respectively, with corresponding minimum VSWR values of 1.32 and 1.29. The maximum DC-to-RF conversion efficiency was 28.85%, while the 1-dB compression output power was 25.0 dBm at 325 MHz.

Thermal measurements showed a maximum device temperature of 54°C at an ambient temperature of 25°C, corresponding to a temperature rise of 29°C. The maximum reported output-power variation was 1.2%, demonstrating stable operation under the tested conditions.

Comparison with the design and simulation values showed relatively small errors, including 1.23% for power gain, 0.76% for output power, 4.44% for input return loss, 2.70% for output return loss, and 3.83% for efficiency. These results provided experimental validation of the developed RF power amplifier and demonstrated the practical relationship between the designed circuit parameters and the measured hardware performance.

4. CONCLUSIONS

A 315–335 MHz RF power amplifier was successfully developed, implemented, and experimentally validated for specialized short-range communication applications. Experimental measurements confirmed operation across the complete

ISSN: 3125-5167, Volume - 1, Issue - 1, 2025
DOI: https://doi.org/10.63456/aamc-1-1-53

20 MHz target frequency range, with the highest power gain of 16.6 dB obtained at 325 MHz. The amplifier delivered a maximum RF output power of 26.0 dBm (0.398 W), while the best input and output return losses were -17.2 dB and -18.0 dB, respectively. The maximum measured DC-to-RF conversion efficiency was 28.85%, demonstrating effective RF power generation relative to DC consumption. Gain-compression testing produced a 1-dB compression output power of 25.0 dBm. Thermal measurements recorded a maximum device temperature of 54°C, while output-power variation remained within 1.2%. Comparison with design and simulation results produced relatively small deviations, thereby experimentally validating the proposed RF design approach and demonstrating its practical suitability for specialized short-range communication systems.

REFERENCES

[1] Akyildiz, I. F., Kak, A., & Nie, S. (2020). 6G and Beyond: The Future of Wireless Communications Systems. *IEEE Access*, *8*, 133995–134030. https://doi.org/10.1109/access.2020.3010896

[2] Anderson, D. A., Sapiro, R. E., & Raithel, G. (2020). An atomic receiver for AM and FM radio communication. *IEEE Transactions on Antennas and Propagation*, *69*(5), 2455–2462. https://doi.org/10.1109/tap.2020.2987112

[3] Cao, F., Liu, L., & Li, L. (2022). Short-wave infrared photodetector. *Materials Today*, *62*, 327–349. https://doi.org/10.1016/j.mattod.2022.11.003

[4] Huang, H., Huang, H., Lin, Y., Cui, S., Huang, Y., Tang, Y., Xu, J., Bao, J., Li, Y., Wen, J., Zuo, H., Wang, W., Li, J., Ni, J., Ruan, Y., Li, L., Chen, Y., Xie, Y., Zhu, Z., . . . Huang, H. (2021). miRTarBase update 2022: an informative resource for experimentally validated miRNA–target interactions. *Nucleic Acids Research*, *50*(D1), D222–D230. https://doi.org/10.1093/nar/gkab1079

[5] Jakubův, J., Chvalovský, K., Goertzel, Z., Kaliszyk, C., Olšák, M., Piotrowski, B., Schulz, S., Suda, M., & Urban, J. (2023). Exploiting generative AI to scale up intelligent tutoring systems. *DROPS (Schloss Dagstuhl – Leibniz Center for Informatics)*. https://doi.org/10.4230/lipics.itp.2023.19

[6] Kodheli, O., Lagunas, E., Maturo, N., Sharma, S. K., Shankar, B., Montoya, J. F. M., Duncan, J. C. M., Spano, D., Chatzinotas, S., Kisseleff, S., Querol, J., Lei, L., Vu, T. X., & Goussetis, G. (2020). Satellite Communications in the New Space Era: A survey and future challenges. *IEEE Communications Surveys & Tutorials*, *23*(1), 70–109. https://doi.org/10.1109/comst.2020.3028247

[7] Lee, G., Park, J., Jang, J., Jung, T., & Kim, T. W. (2019). An IR-UWB CMOS transceiver for High-Data-Rate, Low-Power, and Short-Range communication. *IEEE Journal of Solid-State Circuits*, *54*(8), 2163–2174. https://doi.org/10.1109/jssc.2019.2914584

[8] López, O. L. A., Rosabal, O. M., Ruiz-Guirola, D. E., Raghuwanshi, P., Mikhaylov, K., Lovén, L., & Iyer, S. (2023). Energy-Sustainable IoT connectivity: vision, technological enablers, challenges, and future directions. *IEEE Open Journal of the Communications Society*, *4*, 2609–2666. https://doi.org/10.1109/ojcoms.2023.3323832

[9] Ma, J., Liu, H., Peng, C., & Qiu, T. (2020). Unauthorized Broadcasting Identification: A deep LSTM Recurrent Learning approach. *IEEE Transactions on Instrumentation and Measurement*, *69*(9), 5981–5983. https://doi.org/10.1109/tim.2020.3008988

[10] Vercellone, E. R. (2022). *Design and implementation of wireless nodes for the Internet of Things*. https://doi.org/10.5821/dissertation-2117-367545

[11] Wang, C., You, X., Gao, X., Zhu, X., Li, Z., Zhang, C., Wang, H., Huang, Y., Chen, Y., Haas, H., Thompson, J. S., Larsson, E. G., Di Renzo, M., Tong, W., Zhu, P., Shen, X., Poor, H. V., & Hanzo, L. (2023a). On the Road to 6G: Visions, Requirements, Key Technologies, and Testbeds. *IEEE Communications Surveys & Tutorials*, *25*(2), 905–974. https://doi.org/10.1109/comst.2023.3249835

[12] Wu, Z., Chen, H., Lei, Y., & Xiong, H. (2020). Recognizing automatic link establishment behaviors of a Short-Wave radio station by an improved unidimensional DenseNet. *IEEE Access*, *8*, 96055–96064. https://doi.org/10.1109/access.2020.2997380